doi.org/10.36721/PJPS.2026.39.4.REG.15008.1

Bergapten alleviates Parkinson's disease-like behaviors in mice by inhibiting astrocyte inflammatory activation and endoplasmic reticulum stress through the regulation of the LCN2/JAK2/STAT3 pathway

Jiaxin Li[1#], Rui Tang[1#] and Jiahui Liu[2]*

[1]Department of Neurology, Affiliated Baotou Clinical College of Inner Mongolia Medical University; Baotou City Central Hospital, Baotou, Inner Mongolia, China

[2]Department of Neurology, Baotou Central Hospital, Baotou, Inner Mongolia, China

Abstract: **Background**: Parkinson's disease (PD) is a common neurodegenerative disorder involving multiple pathological processes. Bergapten (BeG) exhibits various pharmacological activities, including anti-inflammatory, antioxidant, and neuroprotective effects, but its mechanism of action in PD remains unclear. **Objective**: This study aimed to investigate the neuroprotective effects and underlying mechanisms of BeG in PD models. **Method**: An *in vitro* neuroinflammation model was established using LPS-treated astrocytes. **Results**: *In-vitro* studies demonstrated that BeG counteracted LPS-induced astrocyte activation by reducing the expressions of GFAP, inflammatory mediators (IL-6, TNF-α, IL-1β), and A1 polarization markers. It alleviated ERS (as indicated by reduced levels of GRP78, CHOP) and apoptosis (as shown by changes in Bax, caspase-3) while enhancing Bcl-2. Mechanistically, BeG suppressed LCN2 expression and JAK2/STAT3 phosphorylation, with LCN2 overexpression attenuating its protective effects. In MPTP-treated mice, BeG improved motor function, preserved dopaminergic neurons, and reduced astrocyte activation and A1 polarization. It increased neurotrophic factors (BDNF, GDNF) while decreasing inflammation, ER stress and apoptotic markers. The inhibition of the LCN2/JAK2/STAT3 pathway was consistently observed in both models, suggesting its central role in BeG's neuroprotective mechanism. **Conclusion**: These findings suggest that BeG exerts neuroprotective effects in PD by inhibiting the LCN2/JAK2/STAT3 signaling pathway, thereby effectively inhibiting astrocyte activation-mediated neuroinflammation and ERS.

Keywords: Astrocytes; Bergapten; Endoplasmic reticulum stress; LCN2/JAK2/STAT3 pathway; Parkinson's disease

Submitted on 12-08-2025 – Revised on 26-09-2025 – Accepted on 13-11-2025

INTRODUCTION

Parkinson's disease (PD) is the second most common neurodegenerative disorder worldwide, affecting nearly six million people globally (Bloem *et al.*, 2021; Dorsey and Bloem, 2024). The disorder is pathologically characterized by two hallmark features: the accumulation of α-synuclein protein aggregates known as Lewy bodies and the selective degeneration of dopaminergic neurons in the substantia nigra. Clinically, patients exhibit characteristic movement disorders including tremors at rest, muscle stiffness, slowed movements and balance impairment, accompanied by various non-motor manifestations such as cognitive impairment, sleep disturbances and reduced olfactory function (Silva *et al.*, 2023). Between 1990 and 2019, the incidence and disability associated with PD demonstrated a marked increase, profoundly affecting patients' daily functioning and creating substantial societal and economic challenges (Ou *et al.*, 2021; Zhong and Zhu, 2022). While existing drug therapies may provide symptomatic relief, they remain ineffective in stopping the progression of the disease (Mulroy *et al.*, 2024; Vijiaratnam *et al.*, 2021). Recent studies suggest that neuroinflammatory mechanisms contribute substantially to the initiation and development of PD, where dysregulated astrocyte activity has been identified as a key driver of neuronal degeneration (Gonzalez-Latapi *et al.*, 2021; Wei and Shetty, 2021).

Astrocytes constitute the predominant glial cell population in the central nervous system (CNS), where they actively release multiple neurotrophic factors and play a critical role in maintaining the stability of the neuronal microenvironment. In disease states, these cells undergo activation, transforming into reactive astrocytes that may differentiate into either pro-inflammatory A1 or neuroprotective A2 subtypes (Ding *et al.*, 2021). Research has shown that A1 astrocytes overexpress complement component C3, secrete large amounts of pro-inflammatory factors and neurotoxic substances and promote dopaminergic neuron damage (Brash-Arias *et al.*, 2024; Wei *et al.*, 2021). The endoplasmic reticulum (ER) is an essential intracellular membrane network that participates in various cellular processes. Its significance in neurodegenerative disorders stems from its essential roles in protein homeostasis, calcium signaling, stress adaptation and autophagic regulation (Liu *et al.*, 2022; Parkkinen *et*

**Corresponding author:* e-mail: LJH6955540@163.com
#These authors are the co-first authors

al., 2023). Research indicates that ER stress (ERS) contributes significantly to PD pathology, where cellular stress triggers the unfolded protein response (UPR). This response subsequently activates apoptotic pathways mediated by key signaling molecules such as ATF6, PERK and IRE1α (Ren *et al.*, 2021). Recent studies have demonstrated that in various CNS disorders, ERS in astrocytes not only affects their own function but also exacerbates neuronal injury through the secretion of inflammatory mediators (Sims *et al.*, 2022).

Lipocalin-2 (LCN2), a pivotal protein in the lipocalin superfamily, was first identified in neutrophil granules and exhibits basal expression across multiple tissues. Importantly, its expression is markedly upregulated in response to pathological stimuli, including tissue damage, microbial infection, or inflammatory challenges (Tan *et al.*, 2024). Experimental studies have shown that either endogenous LCN2 upregulation or exogenous administration of recombinant LCN2 can induce astrocytic activation (Jung *et al.*, 2023). LCN2 functions as a critical mediator in neuroinflammatory processes, where its extracellular release amplifies the synthesis of inflammatory cytokines during stress responses. As a secreted protein, LCN2 has been recognized as a valuable biomarker for assessing neuroinflammatory status, predicting neuronal apoptosis and evaluating cerebral injury (Jung and Ryu, 2023). Mechanistically, LCN2 augments neuroinflammation through specific activation of the Janus kinase 2 (JAK2)-signal transducer and activator of transcription 3 (STAT3) signaling cascade (Wang *et al.*, 2021b). However, the precise mechanisms by which the LCN2/JAK2/STAT3 pathway regulates astrocyte polarization and ERS in PD remain incompletely understood.

Bergapten (BeG) is a naturally occurring furocoumarin compound that is widely found in bergamot essential oil, other citrus essential oils and grapefruit juice (Liang *et al.*, 2021). Mounting studies indicate that BeG demonstrates multiple therapeutic properties through pathway regulation, particularly involving NF-κB, JAK/STAT and PI3K/Akt signaling networks. These mechanisms underlie its observed anti-neuroinflammatory, oxidative stress-reducing and neuron-protecting capacities, which have shown benefits in diverse pathological conditions ranging from fibrotic kidney disease to mood disorders and malignancies (Li *et al.*, 2025a; Perri *et al.*, 2022; Yan *et al.*, 2023). Nevertheless, the potential therapeutic effects of BeG in PD pathogenesis await further investigation. This study aims to explore the mechanism by which BeG regulates astrocyte activation and ERS in PD by targeting the LCN2/JAK2/STAT3 pathway. These results may contribute novel mechanistic understanding for mitigating PD advancement while serving as a valuable foundation for identifying promising therapeutic agents against PD.

MATERIALS AND METHODS

Cell culture and transfection

In this investigation, the C8-D1A murine astrocyte cell line was obtained from the Chinese Academy of Sciences Cell Bank (Shanghai, China) and maintained in specialized growth medium (MD156) at standard culture conditions (37°C, 5% CO_2 atmosphere).

To investigate the biological function of LCN2, a pcDNA3.1-LCN2 overexpression plasmid was constructed. This plasmid was commercially synthesized by Sangon Biotech (Shanghai, China) using the pcDNA3.1(+) vector as the backbone and was sequence-verified before transfection. The verified plasmid was then transfected into target cells using Lipofectamine 3000 transfection reagent to establish a stable LCN2 overexpression cell model. The specific transfection procedure was as follows: The C8-D1A astrocytes were plated in 6-well culture dishes and allowed to grow until reaching 70-80% confluence. Transfection was then carried out in strict accordance with the manufacturer's protocol for Lipofectamine 3000 (L3000150, Invitrogen). 6 h post-transfection, the culture medium was refreshed before initiating further experimental procedures.

Cell treatment

The study initially evaluated the cytotoxicity profile of BeG (CAS 484-20-8, TargetMol; molecular structure shown in Fig. 1A) through CCK-8 viability assays to establish appropriate dosing parameters. Astrocyte cultures were exposed to a concentration gradient of BeG (1.25, 5, 10, 20, 40, 80 μM) for 24-48 h to identify non-toxic treatment ranges. To establish the neuroinflammatory model, astrocytes were maintained in culture medium supplemented with 100 ng/mL lipopolysaccharides (LPS, SMB00704, Sigma) for a 24 h period (Pierre *et al.*, 2022). Following a 2 h pretreatment with varying doses of BeG, cell viability was quantitatively assessed through CCK-8 colorimetric analysis. Based on preliminary screening, BeG at 5, 10, 20 μM effectively protected against LPS-induced cytotoxicity and was therefore used for further studies. The experiment included: (1) untreated controls, (2) LPS-treated cells and (3) LPS + BeG (5, 10, 20 μM) groups to examine BeG's dose-dependent effects on astrocyte activation, A1 polarization, ER stress and apoptosis.

To elucidate BeG's mechanism in preventing LPS-induced A1 polarization via ERS modulation, five treatment conditions were established: (1) untreated controls; (2) LPS alone; (3) LPS with 20 μM BeG; (4) LPS plus 5 mM 4-PBA (ERS inhibitor, P-21005, Sigma), with 1 h 4-PBA pretreatment before LPS exposure; and (5) LPS combined with both 20 μM BeG and 0.1 μM TG (ERS activator, T9033, Sigma), involving 2 h pretreatment with TG/BeG prior to LPS stimulation (Yang *et al.*, 2024).

To investigate whether BeG's protective effects against LPS-induced astrocyte activation, A1 polarization and ER stress involve the LCN2/JAK2/STAT3 pathway, we performed LCN2 gain-of-function experiments. Astrocytes were transfected with either LCN2 overexpression construct (OE-LCN2) or empty vector control (OE-NC), followed by treatment with: (1) vehicle control, (2) LPS alone, (3) LPS+20μM BeG, (4) LPS+BeG+OE-NC, or (5) LPS+BeG+OE-LCN2. This approach enabled assessment of how LCN2 overexpression modulates BeG's neuroprotective actions.

Cell viability

Cell viability was determined by CCK-8 assay (C0037, Beyotime). Briefly, cells were plated in 96-well plates (100 μL medium/well) and treated as per the experimental design. Following interventions, 10 μL CCK-8 reagent was added to each well and cells were incubated for 3 h (37°C). The optical density at 450 nm was quantified using a microplate reader (Benchmark, Bio-Rad) to calculate viability percentages.

Lactate dehydrogenase (LDH) release

LDH release serves as a biomarker of membrane integrity, providing an indirect measure of cellular damage. For this assay, cells were cultured in 96-well plates and subjected to the designated experimental treatments. Following intervention, culture supernatants were harvested by centrifugation (400 g, 5 min) and analyzed using a commercial LDH detection kit (C0016, Beyotime) according to manufacturer specifications. The optical density at 490 nm was determined spectrophotometrically, enabling calculation of LDH release rates.

Flow cytometry

Cell apoptosis was quantitatively analyzed through Annexin V-APC/PI dual staining (88-8007-74, Invitrogen). Following experimental treatments, harvested cells were PBS-washed and processed as follows: 5×10^5 cells/mL were suspended in 200 μL binding buffer, with 195 μL aliquots incubated with 5 μL Annexin V-APC (dark, RT, 10 min). After washing, cells were resuspended in 190 μL binding buffer containing 10 μL PI (20 μg/mL). Analysis was performed using a flow cytometer (BD FACSCanto II, BD Biosciences) and data were processed using FlowJo software.

Animals and treatment

Thirty-five 8-week-old male C57BL/6 mice (weighing 22–25 g) were acclimated for one week in a controlled environment (22±2°C, 55±10% humidity) with a 12 h light/dark cycle. Throughout the study, animals had ad libitum access to autoclaved food and water.

The PD model was induced in mice through intraperitoneal administration of MPTP-HCl (20 mg/kg; M0896, Sigma) administered four times at 2 h intervals. Behavioral assessments were conducted 7 days post-injection (Fan *et al.*, 2021). Control animals received equal volumes of saline. For therapeutic intervention, mice received BeG pretreatment (3, 10, or 30 mg/kg, i.p.) 12 h prior to MPTP administration, followed by once-daily dosing for 4 consecutive days post-modeling (Yan *et al.*, 2023). The saline group received an equivalent volume of solvent injection.

Behavioral testing

Behavioral tests were conducted one day before euthanasia, with pre-training performed daily for three consecutive days prior to testing. All behavioral tests were conducted by two experienced investigators who were blinded to the group assignments.

Open field test (Song *et al.*, 2021): The experimental setup consisted of a 50 cm × 50 cm × 50 cm enclosed chamber. Mice were acclimated to the environment before the test and their behavior was recorded for approximately 5 min. Between each group's test, the chamber was wiped with 70% ethanol to eliminate odor interference. The total distance traveled (mm) was analyzed using video recordings.

Pole test (Qiao *et al.*, 2025): The motor coordination of mice was evaluated using a vertical pole apparatus (55 cm length × 1 cm diameter) wrapped with textured gauze to enhance grip. Each mouse was placed head-up at the pole's apex and the descent latency was recorded from initial forepaw contact until complete hindlimb detachment. Three trials were conducted per animal at 15-min intervals, with the mean descent duration used for statistical analysis.

Rotarod test (Haque *et al.*, 2021): Mice were trained on a rotarod device at 4 rpm for 300 s daily for 3 consecutive days. During testing, mice were placed on an accelerating rod from 4 rpm to 40 rpm and the time until they fell was recorded. Three consecutive tests were performed with 15 min intervals and the average time was used for data analysis.

Terminal deoxynucleotidyl transferase dUTP nick-end labeling (TUNEL) staining

Apoptosis levels in mouse astrocytes and brain tissues were detected using TUNEL staining. Astrocytes were rinsed with PBS, fixed using 4% PFA and treated with permeabilization buffer for 5 min. Mouse brain tissue samples underwent fixation, dehydration, paraffin embedding and sectioning. Apoptotic cells were detected using a TUNEL assay (HY-K1078, MCE) according to the manufacturer's protocol. Briefly, 50 μL of TUNEL reaction mixture was applied to the samples, which were then incubated at 37°C for 60 min under light-protected conditions. Observations and imaging were conducted under a fluorescence microscope (DMi8, Leica) and TUNEL-positive cells were counted and analyzed using ImageJ software (version 1.54p).

Enzyme-linked immunosorbent assay (ELISA)

To quantify cytokine and neurotrophic factor levels in the supernatant of mouse astrocyte cultures and brain tissue homogenates, samples were homogenized ultrasonically and centrifuged (12,000 rpm, 20 min, 4°C) to collect the supernatant. The concentrations of Nitric oxide (NO, MBS2608310, MyBiosource), IL-6 (MBS2508516, MyBiosource), TNF-α (MBS494101, MyBiosource), IL-1β (RAB0275, Sigma), BDNF (MBS9135966, MyBiosource) and GDNF (MBS494778, MyBiosource) in mouse cells or brain tissues were quantified using commercial ELISA kits following the manufacturers' protocols. Absorbance readings were obtained with a microplate reader (Multiskan GO, Thermo) and analyte concentrations were determined using standard curves.

Immunofluorescence

Following treatment, C8-D1A cells were fixed in 4% PFA and permeabilized using 0.2% Triton X-100. For tissue processing, mouse brains were fixed in 4% PFA, dehydrated through an ethanol gradient, cleared in xylene and paraffin-embedded (60 min). Sections (6μm thickness) were obtained using a microtome. For immunostaining, samples were blocked with 5% goat serum (BL210A, Biosharp; 1h, RT) before incubation with primary antibodies targeting: C3 (1:50, ab321966, Abcam), S100A10 (5 μg/mL, PA5-95505, Invitrogen), GRP78 (5 μg/mL, ab21685, Abcam), TH (1:100, ab137869, Abcam), LCN2 (1:50, PA5-116955, Invitrogen) and GFAP (1:100, #80788, CST) at 4°C overnight. After PBS washes, samples were incubated with species-matched fluorescent secondary antibodies (1:500, ab150077/ab150080, Abcam; 37°C, 30 min). Nuclei were visualized with DAPI counterstain (C1002, Beyotime). Images were acquired via fluorescence microscopy and ImageJ was employed for cell counting and co-localization analysis of positively labeled cells.

Western blot

Protein extraction was performed by lysing cells or brain tissues in RIPA buffer (R0010, Solarbio) followed by centrifugation (13,000 rpm, 10 min, 4°C) to obtain soluble fractions. Protein concentrations were quantified using a BCA assay (BL521A, Biosharp). Equal amounts of protein (30 μg/lane) were resolved by SDS-PAGE and subsequently electrotransferred to PVDF membranes (BS-PVDF-45, Biosharp). After blocking with 5% skim milk, membranes were incubated with primary antibodies against GFAP (1:1000, #80788, CST), iNOS (1:1000, ab178945, Abcam), COX2 (1:2000, ab179800, Abcam), C3 (1:1000, ab321966, Abcam), S100A10 (0.5 μg/mL, PA5-95505, Invitrogen), LCN2 (1:1000, ab216462, Abcam), p-JAK2 (1:5000, ab32101, Abcam), JAK2 (1:5000, ab108596, Abcam), p-STAT3 (1:5000, ab76315, Abcam), STAT3 (1:1000, ab68153, Abcam), CHOP (1:1000, #2895, CST), GRP78 (1 μg/mL, ab21685, Abcam), IRE1α (1:1000, ab322061, Abcam), p-IRE1α (1:1000, ab48187, Abcam), PERK (1:1000, ab229912, Abcam), p-PERK (1:500, PA5-40294, Invitrogen), Bax (1:1000, #2772, CST), Bcl2 (1:1000, #3498, CST), caspase-3 (1:1000, #9662, CST), cleaved-caspase-3 (1:1000, #9661, CST), caspase-12 (1 μg/mL, PA5-19963, Invitrogen), TH (1:5000, ab137869, Abcam) and GAPDH (1:1000, #2118, CST) at 4°C overnight. Following overnight incubation and TBST washes, membranes were probed with HRP-conjugated goat anti-rabbit IgG secondary antibody (1:20,000 dilution; ab97051, Abcam) for 1 h at room temperature. Protein signals were detected using an ECL substrate (E412-01, Vazyme) and captured with a Tanon 5200 imaging system. Band intensities were quantified through grayscale analysis using ImageJ software. GAPDH was used as an internal control for normalization.

Statistical analysis

All experimental data are presented as mean ± SEM. Data was subjected to the Normality test and Levene's test of Homogeneity of Variance. Statistical comparisons among test groups were made using one-way ANOVA with Tukey's post-hoc analysis (SPSS 27.0), as the experimental design included more than two groups, rendering the Student's t-test inappropriate. For Western blot and flow cytometry data that were not normally distributed, the non-parametric Mann-Whitney U test was used. Data visualization was conducted using GraphPad Prism 10.1, with statistical significance set at $p < 0.05$.

RESULTS

BeG inhibits LPS-induced astrocyte activation

This study initially assessed the effect of different concentrations of BeG on the viability of mouse astrocytes using the CCK-8 assay system. BeG demonstrated no significant cytotoxic effects on astrocytes at concentrations ranging from 1.25, 5, 10 and 20 μM during the 24/48 h treatment period. However, marked reductions in cell viability became apparent at concentrations of 40 and 80 μM (Fig. 1B). In the LPS-induced inflammation model, astrocyte viability was significantly decreased, whereas treatment with 5, 10, 20 and 40 μM BeG significantly increased cell viability (Fig. 1C). Based on these results, we selected 5, 10 and 20 μM, which are both safe and effective concentrations, for subsequent experiments to ensure the reliability of the results.

In order to investigate BeG's modulatory effects on LPS-induced astrocyte activation and elucidate its underlying mechanisms, we established five experimental groups: (1) control, (2) LPS-treated, (3) LPS with 5 μM BeG cotreatment, (4) LPS with 10 μM BeG cotreatment and (5) LPS with 20 μM BeG cotreatment. The LDH release assay results showed that LPS-induced astrocytes exhibited

significantly elevated LDH release, indicating that LPS could cause astrocyte damage. BeG intervention, however, significantly inhibited LDH release in a dose-dependent manner (Fig. 1D). GFAP is a specific marker of astrocyte activation (Jurga *et al.*, 2021) and consistent results from GFAP immunofluorescence and Western blotting showed that LPS treatment significantly upregulated GFAP protein expression in astrocytes, while BeG treatment dose-dependently downregulated GFAP protein expression (Fig. 1E-H). These findings demonstrate that BeG exerts protective effects against LPS-induced cellular injury while suppressing astrocyte activation.

NO has a dual role in PD, as it can exacerbate neurodegeneration through oxidative damage and inflammation, but may also exert neuroprotective effects at low concentrations (Tripodi *et al.*, 2025). Meanwhile, pro-inflammatory cytokines exacerbate neuroinflammation and promote neuronal damage and death, which are key drivers of neurodegenerative changes in PD (Qu *et al.*, 2023). LPS treatment significantly upregulated the secretion of inflammatory markers NO, IL-6, TNF-α and IL-1β in astrocyte cultures, as quantified by ELISA (Fig. 1I-L), verifying robust inflammatory activation. BeG treatment exhibited concentration-dependent suppression of pro-inflammatory cytokine secretion and inflammatory mediators, effectively attenuating LPS-induced neuroinflammatory responses in astrocytes. Protein analysis confirmed LPS-mediated upregulation of iNOS and COX2 expression, while BeG administration dose-dependently attenuated these inflammatory markers (Fig. 1M-N). Given the established role of iNOS and COX2 as central mediators in neuroinflammation (Rauf *et al.*, 2022), their pharmacological inhibition represents an effective strategy for reducing downstream inflammatory molecules like NO (Subedi *et al.*, 2021), resulting in attenuated neuroinflammatory pathology.

BeG inhibits LPS-induced astrocyte A1 polarization

C3 and S100A10 represent functionally significant astrocyte markers, with C3 promoting neuroinflammation via complement activation and S100A10 coordinating glial responses during inflammation and repair (Boulton and Al-Rubaie, 2025). C3 specifically labels pro-inflammatory A1-type astrocytes, while S100A10 specifically labels neuroprotective A2-type astrocytes. Therefore, C3/GFAP co-expression is commonly used to identify A1-type astrocytes and S100A10/GFAP co-expression is used to detect A2-type astrocytes (Pang *et al.*, 2021). Combined immunofluorescence and Western blot analyses were employed to assess BeG's regulatory influence on LPS-induced astrocyte polarization. Immunofluorescence analysis revealed LPS-induced astrocyte polarization, characterized by increased $GFAP^{+}/C3^{+}$ A1 phenotype frequency concomitant with decreased $GFAP^{+}/S100A10^{+}$ A2 subpopulation (Fig. 2A-D). BeG treatment demonstrated concentration-dependent modulation of this polarization shift, effectively suppressing A1-type activation while promoting A2-type predominance. Western blot analysis further confirmed this result. After LPS treatment, the C3 protein level in astrocytes was significantly upregulated, while the S100A10 protein level was significantly downregulated. BeG intervention effectively regulated the expression of these two proteins (Figs. 2E-G). The data support a potential therapeutic mechanism whereby BeG confers neuroprotection by rebalancing astrocyte polarization states, inhibiting detrimental A1 activation and promoting beneficial A2 characteristics.

BeG inhibits LPS-induced astrocyte ERS and cell apoptosis

GRP78, an HSP70 family member, serves as a central regulator of ERS responses. As the primary molecular chaperone within the ER lumen, its expression is markedly upregulated under cellular stress conditions (Nourbakhsh *et al.*, 2022). Immunofluorescence quantification revealed LPS-induced upregulation of the ERS marker GRP78 in $GFAP^{+}$ astrocytes, while BeG treatment produced a concentration-dependent attenuation of GRP78 expression (Fig. 3A-B). In addition, IRE1α and PERK are two signaling molecules that play key roles in the ERS process. The canonical ERS pathway involves sequential PERK activation, eIF2α phosphorylation and ATF4-dependent CHOP induction (Li *et al.*, 2025b). Western blot quantification revealed BeG's concentration-dependent inhibition of this signaling network, significantly lowering both terminal effectors (CHOP, GRP78) and upstream regulators (p-IRE1α, p-PERK) in the stress response pathways (Fig. 3C-D). These results support BeG's capacity to attenuate LPS-mediated cellular stress by targeting ERS signaling mechanisms.

Consistent results from TUNEL assays and flow cytometry revealed a marked increase in apoptotic rates among astrocytes after LPS treatment, suggesting that LPS triggers apoptosis in these cells (Fig. 3E-H). BeG treatment significantly reduced LPS-induced astrocyte apoptosis. Western blotting revealed that LPS exposure upregulated Bax, caspase-12 and the cleaved-caspase-3/caspase-3 ratio but downregulated Bcl-2 in astrocytes. In contrast, BeG treatment dose-dependently increased Bcl-2 expression while reducing the levels of these pro-apoptotic proteins (Fig. 3I-J). These results suggest that BeG exerts its anti-apoptotic effects through inhibition of both the ERS-related apoptotic pathway (involving CHOP and caspase-12) and the mitochondrial apoptotic pathway (mediated by Bcl-2, Bax, and caspase-3).

BeG attenuates LPS-induced astrocyte A1 polarization by inhibiting ERS

To elucidate the role of ERS in BeG-mediated astrocyte polarization, pharmacological interventions were

employed using the ER inhibitor 4-PBA and ER agonist TG. Immunofluorescence and immunoblotting analyses demonstrated that 4-PBA treatment following LPS exposure resulted in significant suppression of the A1 phenotype marker C3 concurrent with marked elevation of the A2 marker S100A10, relative to LPS treatment alone. This suggests that LPS can induce astrocyte A1 polarization and that this pathway is associated with the activation of ERS. Protein expression profiling revealed that 20 μM BeG treatment produced comparable modulatory effects on C3 and S100A10 expression patterns as observed with 4-PBA intervention, suggesting BeG's capacity to suppress LPS-induced ERS. This inhibitory effect was further substantiated through co-treatment experiments with the ER stress inducer TG, which effectively counteracted BeG-mediated regulation in the LPS-challenged cellular model. Immunophenotyping results indicated that both therapeutic agents mediated a phenotypic shift in astrocyte populations, with quantitative reductions in neurotoxic A1-type cells and proportional increases in neuroprotective A2-type cells (Fig. 4A-F). These results indicate that BeG can attenuate LPS-induced astrocyte A1 polarization and promote neuroprotective A2 polarization by inhibiting ERS. The inflammatory cytokine analysis showed that BeG and 4-PBA comparably inhibited the release of key pro-inflammatory factors (IL-1β, IL-6, TNF-α) in LPS-activated cells and this effect was antagonized by TG (Fig. 4G-I). Our results establish that BeG's mechanism of action involves targeted interference with ERS-dependent astrocyte polarization, effectively attenuating both A1 phenotypic conversion and its related inflammatory cascade.

BeG inhibits the LPS-induced LCN2/JAK2/STAT3 signaling pathway in astrocytes

Investigations have revealed that LCN2, an important astrocytic factor, functions as a neuroinflammatory regulator through JAK2/STAT3 signaling activation, with significant implications for both pathological inflammation and restorative processes (Han *et al.*, 2024; Song *et al.*, 2025). To elucidate the neuroprotective mechanism of BeG, this study focuses on its regulatory effects on the LCN2/JAK2/STAT3 pathway. Immunofluorescence detection revealed that LPS stimulation significantly enhanced the co-expression of LCN2 and GFAP in astrocytes, whereas BeG treatment dose-dependently inhibited this co-expression (Fig. 5A-B). Protein analysis revealed that LPS exposure significantly elevated both LCN2 levels and JAK2/STAT3 activation (phosphorylation) in astrocytes, effects that were progressively counteracted by increasing concentrations of BeG (Fig. 5C-D). The experimental evidence suggests that BeG exerts its inhibitory effects on astrocyte activation primarily by targeting the LCN2/JAK2/STAT3 signaling axis.

To comprehensively elucidate BeG's regulatory role and underlying mechanisms in the LCN2/JAK2/STAT3 pathway, we established an LCN2-overexpressing cellular model for systematic investigation. Protein expression analysis confirmed successful LCN2 overexpression, with significantly elevated LCN2 levels in the OE-LCN2 group compared to empty vector controls (OE-NC) (Fig. 5E-F). Western blot analysis revealed that BeG treatment significantly downregulated the phosphorylation levels of JAK2 and STAT3 (Fig. 5G-H) and LCN2 overexpression markedly reversed the inhibitory effect of BeG on JAK2/STAT3 phosphorylation. These results demonstrate that BeG mediates its suppression of JAK2/STAT3 signaling primarily through LCN2 downregulation in LPS-stimulated astrocytes.

BeG inhibits LPS-induced astrocyte activation, A1 polarization and ERS by regulating the LCN2/JAK2/STAT3 pathway

The experimental data demonstrated that forced LCN2 expression (OE-LCN2) in BeG-treated samples significantly increased both the population of A1-polarized astrocytes and C3 protein levels compared to BeG treatment alone (Fig. 6A-D). These findings establish that BeG modulates astrocyte polarization via LCN2-dependent mechanisms. Additionally, ELISA and Western blot results confirmed that the anti-inflammatory activity of BeG was significantly reversed by LCN2 overexpression, with the LPS+BeG+OE-LCN2 group showing marked upregulation of both cytokine production (IL-1β, IL-6, TNF-α) and inflammatory proteins (iNOS, COX2) relative to BeG-only treatment (Fig. 6E-I). These findings further confirm that BeG inhibits the expression of LCN2, thereby inhibiting the activation of downstream inflammatory signaling pathways and ultimately inhibiting astrocyte A1 polarization and neuroinflammatory responses.

The immunostaining results revealed a significant increase in GFAP and GRP78 co-localization following LPS treatment, which was notably suppressed by BeG intervention (Fig. 6J-K), suggesting BeG's capacity to ameliorate ERS in activated astrocytes. The Western blot analysis further verified that BeG markedly reduced the levels of critical ERS markers (GRP78, CHOP) in LPS-stimulated astrocytes, while also suppressing the activation of both IRE1α and PERK signaling pathways through decreased phosphorylation (Fig. 6L-M). Notably, BeG promoted the upregulation of Bcl-2, an anti-apoptotic factor, while concurrently downregulating pro-apoptotic proteins such as Bax and caspase-12, as well as the cleaved-caspase-3/caspase-3 activation ratio (Fig. 6N-O). Overexpression of LCN2 significantly reversed the inhibitory effect of BeG on ERS as well as its anti-apoptotic effect. Overall, the results establish that BeG's neuroprotective effects are mediated via inhibition of the LCN2/JAK2/STAT3 axis, which in turn mitigates astrocyte

activation, attenuates A1 polarization and dampens ERS responses.

BeG inhibits astrocyte activation and A1 polarization in MPTP-induced PD mice

This study utilized the MPTP-induced PD mouse model, setting up five experimental groups: Saline group, MPTP model group and MPTP combined with different doses of BeG treatment groups (3, 10, 30 mg/kg), to systematically evaluate the neuroprotective effects of BeG. Motor function analyses indicated that MPTP administration caused significant behavioral abnormalities compared to the saline group, characterized by: shorter travel distance in open field experiments, increased time-to-descend in pole tests and impaired performance on rotating rods. These MPTP-induced motor deficits were progressively reversed by BeG treatment across tested doses, achieving optimal efficacy at 30 mg/kg (Fig. 7A-C).

As TH serves as a specific marker for dopaminergic neurons, its decreased expression in PD models reflects both neuronal loss and concomitant glial hyperactivation (Gao *et al.*, 2022; Yang and Zhuang, 2025). Fluorescent immunohistochemical analysis identified characteristic PD-like neuropathology in MPTP models, featuring both reactive astrogliosis (enhanced $GFAP^+$ red signal) and dopaminergic neurodegeneration (diminished TH^+ green signal) when compared to saline control specimens (Fig. 7D-F). Western blot results further confirmed this trend (Fig. 7G-H). BeG treatment groups at all doses were able to dose-dependently inhibit GFAP overexpression and protect TH-positive neurons, with the 30 mg/kg group showing the best effect. Quantitative ELISA measurements identified substantial decreases in both BDNF and GDNF levels in MPTP model mice relative to the saline group, while BeG treatment progressively normalized these neurotrophic markers across increasing dosage regimens (Fig. 7I-J).

Astrocyte phenotype analysis revealed that MPTP administration promoted A1 polarization ($C3^+/GFAP^+$) while suppressing A2 markers ($S100A10^+/GFAP^+$), alterations that were ameliorated by BeG intervention (Fig. 7K-M). Quantitative analysis demonstrated MPTP-induced upregulation of pro-inflammatory cytokines (IL-6, IL-1β, TNF-α) in brain tissue, which was progressively attenuated by graded doses of BeG (Fig. 7N-P). These experimental results reveal that BeG's neuroprotective properties are mediated through several distinct targets: improving motor dysfunction at the behavioral level, inhibiting astrocyte activation and protecting dopaminergic neurons at the cellular level and regulating neurotrophic factor secretion, improving astrocyte polarization and inhibiting neuroinflammation at the molecular level. Among these, the 30 mg/kg dose group demonstrated the best protective effects across all indicators.

BeG alleviates neuroinflammatory stress in MPTP-induced PD mice by inhibiting the LCN2/JAK2/STAT3 signaling pathway

Using an MPTP-induced PD murine model, this investigation explored BeG's modulation of the LCN2/JAK2/STAT3 pathway. Immunohistochemical and immunoblotting analyses demonstrated marked elevation of LCN2 expression and enhanced JAK2/STAT3 phosphorylation in MPTP-treated animals relative to saline controls (Fig. 8A-D). BeG treatment dose-dependently suppressed LCN2 overexpression, with maximal inhibition of JAK2/STAT3 phosphorylation observed at 30 mg/kg.

Immunofluorescence analysis demonstrated MPTP-induced upregulation of GFAP/GRP78 double-positive cells (Fig. 8E-F), while TUNEL staining confirmed enhanced apoptotic rate relative to saline-treated animals (Fig. 8G-H). Immunoblot analysis demonstrated upregulation of ERS markers (CHOP and GRP78) and enhanced phosphorylation of IRE1α and PERK in MPTP-treated brain tissue (Fig. 8I-J). Concurrently, we observed elevated expression of pro-apoptotic factors (Bax and caspase-12), increased caspase-3 activation and downregulation of Bcl-2 (Fig. 8K-L). BeG treatment dose-dependently improved these abnormal changes, with the 30 mg/kg group showing the best results. These results confirm that BeG exerts neuroprotective effects against MPTP-induced PD in mice by inhibiting the activation of the LCN2/JAK2/STAT3 signaling pathway, thereby alleviating neuroinflammatory responses, mitigating ERS and suppressing cell apoptosis.

DISCUSSION

PD is a progressive neurodegenerative disorder primarily involving dopaminergic neuron degeneration in the substantia nigra and Lewy body formation, which clinically manifests as characteristic motor impairments including resting tremor, bradykinesia, rigidity and postural instability (Chen *et al.*, 2025). During disease progression, PD patients frequently develop various non-motor manifestations including cognitive decline, sleep disorders and depressive symptoms that significantly compromise their daily functioning and life quality (Su *et al.*, 2021). PD arises from multiple interacting factors, including genetic susceptibility, environmental triggers and dysregulated cellular processes such as α-synuclein accumulation, oxidative damage, mitochondrial impairment and neuroinflammation (Kim *et al.*, 2023). Currently, treatment for PD mainly focuses on pharmacological management, such as levodopa replacement therapy, but these treatments cannot halt disease progression and long-term use leads to side effects (Kwon *et al.*, 2022). Thus, further investigation into PD's underlying mechanisms and the discovery of interventions that can modify disease course by protecting vulnerable neurons remains an important research priority for improving clinical prognosis.

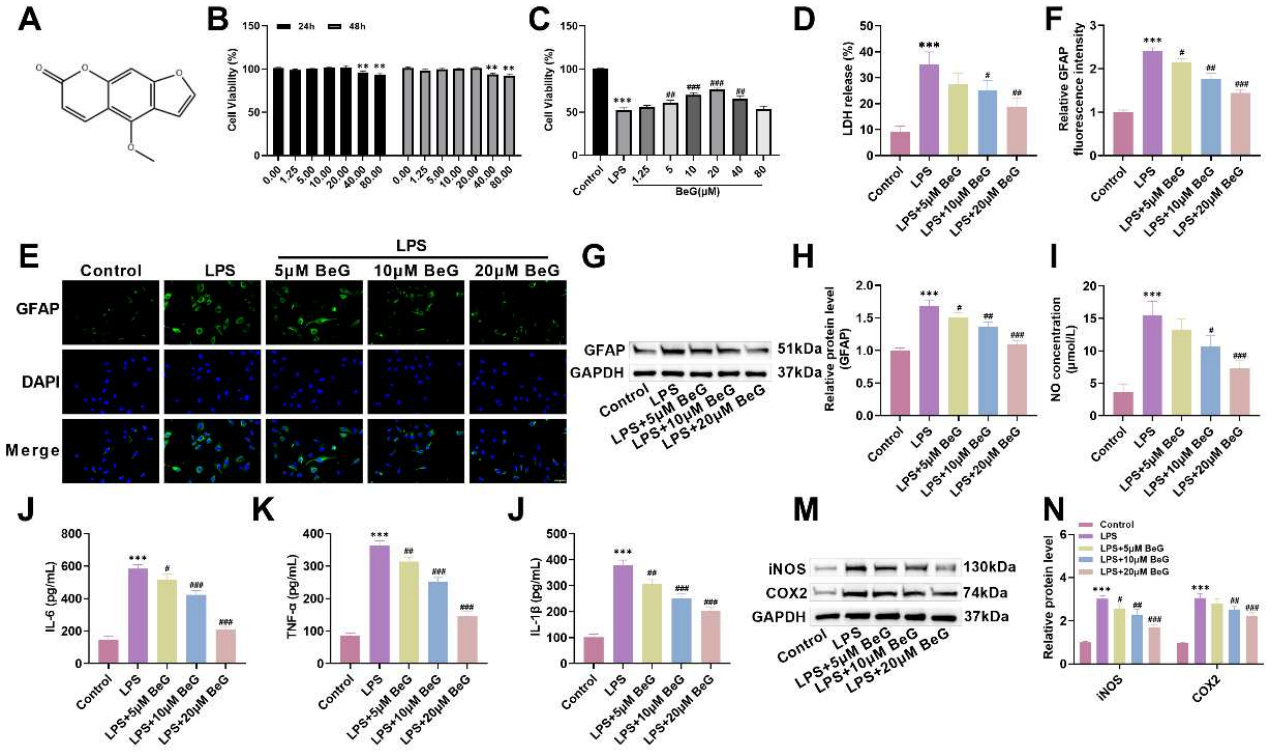

Fig. 1: BeG inhibits LPS-induced astrocyte activation.
(A) Chemical structure of BeG. (B-C) Cell viability was measured by CCK-8 assay in astrocytes treated with BeG (0, 1.25, 5, 10, 20, 40, 80 μM) for 24 h, either alone or following LPS challenge. The optimal concentrations (5, 10, 20 μM) were selected for further experiments. (D) Experimental groups included: Control, LPS, and LPS+BeG (5/10/20 μM). LDH release assay assessed cellular damage. (E-F) GFAP immunofluorescence evaluated astrocyte activation. Scale bar 50 μm. (G-H) GFAP protein levels were confirmed by immunoblotting. (I-L) Secreted inflammatory mediators (NO, IL-6, TNF-α, IL-1β) were quantified by ELISA. (M-N) Inflammatory markers (iNOS, COX2) were analyzed by immunoblotting. n=3. ** P<0.01, *** P<0.001 vs Control; # P<0.05, ## P<0.01, ### P<0.001 vs LPS.

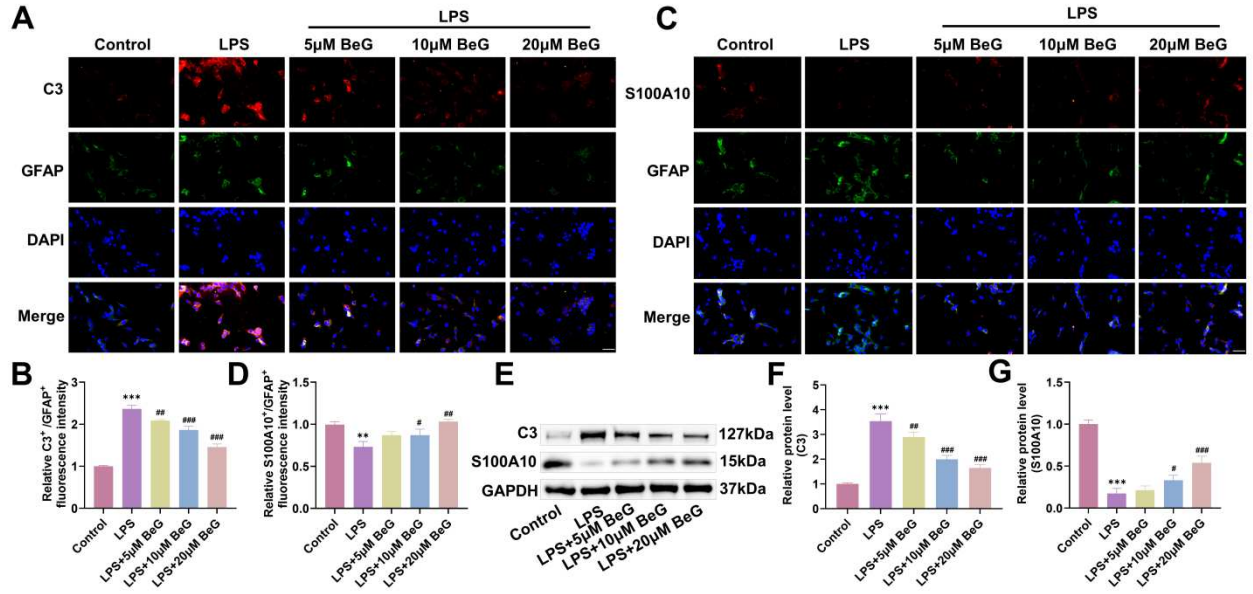

Fig. 2: BeG inhibits LPS-induced astrocyte A1 polarization.
(A-D) Immunofluorescence analysis of astrocyte polarization markers (A1: GFAP$^+$/C3$^+$; A2: GFAP$^+$/S100A10$^+$) evaluated BeG's modulation of LPS-induced phenotypic shifts. Scale bar 50 μm. (E-G) Immunoblotting quantified A1/A2 polarization markers (C3, S100A10) to validate BeG's regulatory effects. n=3. ** P<0.01, *** P<0.001 vs Control; # P<0.05, ## P<0.01, ### P<0.001 vs LPS.

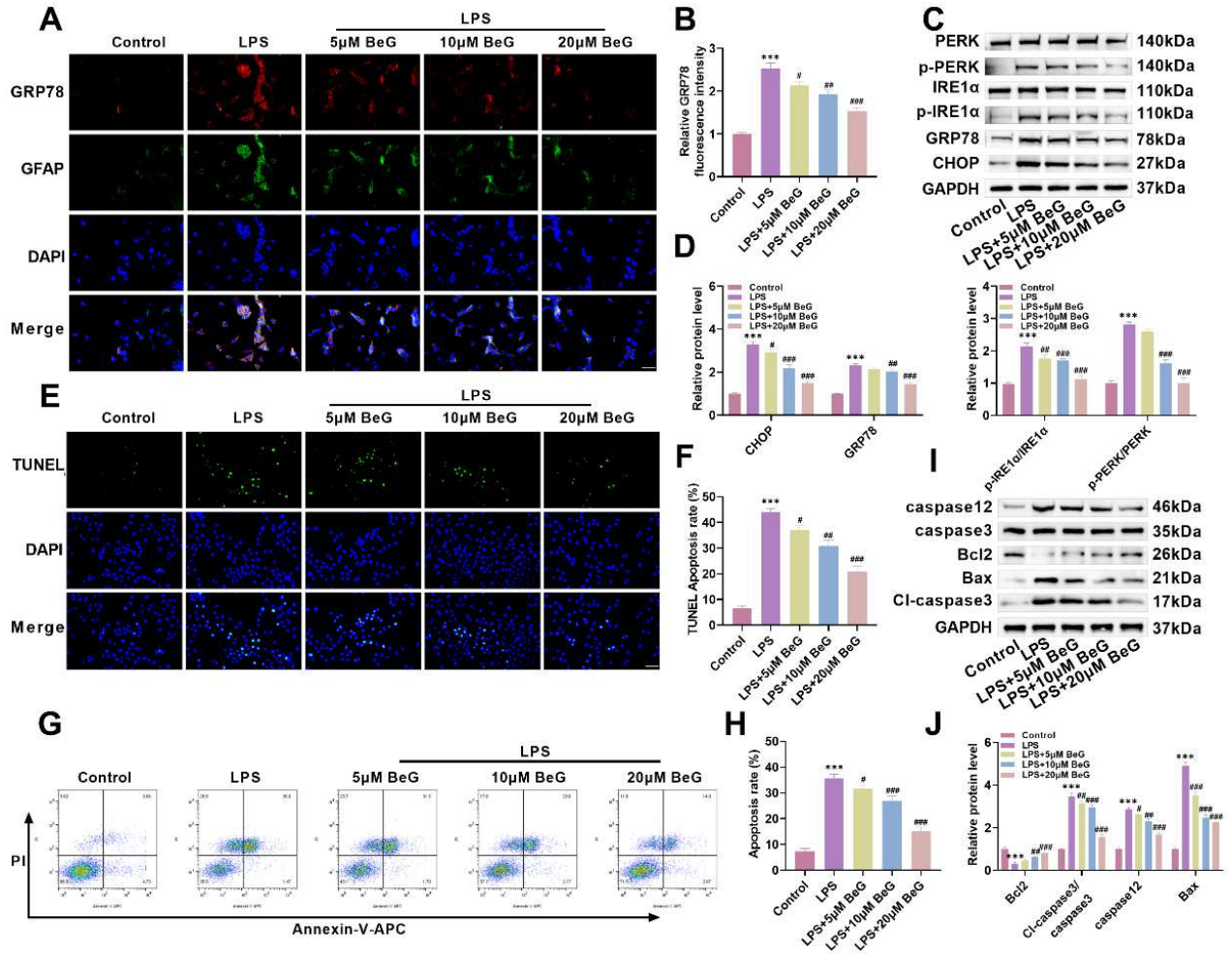

Fig. 3: BeG inhibits LPS-induced astrocyte ERS and cell apoptosis.
(A-B) Immunofluorescence colocalization of GRP78/GFAP assessed BeG's modulation of LPS-induced astrocyte activation and ER stress. Scale bar 50 μm. (C-D) Immunoblot analysis of ER stress markers (CHOP, GRP78, IRE1α/p-IRE1α, PERK/p-PERK) further elucidated BeG's protective effects. (E-F) TUNEL staining quantified apoptotic rates across treatment groups. Scale bar 50 μm. (G-H) Flow cytometry validated apoptosis levels. (I-J) Immunoblotting of apoptotic regulators (Bax, Bcl-2, caspase-3/cleaved-caspase-3, caspase-12) clarified BeG's antiapoptotic mechanism. n=3. *** P<0.001 vs Control; # P<0.05, ## P<0.01, ### P<0.001 vs LPS.

The MPTP-induced PD model displayed significant motor dysfunction, with reduced exploratory distance, delayed descent and diminished balance retention. Importantly, BeG administration demonstrated dose-dependent amelioration of motor impairments in PD mice, with optimal efficacy observed at 30 mg/kg. Recent studies have highlighted the pivotal role of neuroinflammation in both the initiation and advancement of PD.

This inflammatory process within the CNS is characterized by dysregulated activation of resident immune cells, particularly microglia and astrocytes (Jurcau *et al.*, 2023). As the predominant glial population, astrocytes are essential for CNS homeostasis through their diverse functions in neuronal support, synaptic modulation and immune regulation (Hart and Karimi-Abdolrezaee, 2021; Lee *et al.*, 2022). Under pathological conditions such as PD, however, these cells undergo reactive transformation accompanied by profound morphological and functional alterations (Dong *et al.*, 2023). This study found that LPS stimulation significantly induced astrocyte activation and cell damage, manifested by a marked upregulation of GFAP expression and a significant increase in LDH release. LPS stimulation triggered the release of pro-inflammatory cytokines (IL-6, TNF-α, IL-1β) and elevated inflammatory mediators (iNOS, COX2), confirming neuroinflammatory progression. BeG treatment effectively suppressed LPS-induced astrocyte activation in a dose-dependent manner, mitigating cellular damage and reducing inflammatory markers. Similarly, *in vivo*, MPTP administration increased $GFAP^+$ astrocytes while decreasing TH^+ dopaminergic neurons, aligning with the LPS-induced neuroinflammatory response. Significant neuroprotection was observed following BeG treatment, as evidenced by reduced GFAP levels and maintained TH-positive neuron integrity, suggesting its therapeutic potential in modulating astrocyte reactivity and dopaminergic neuron survival.

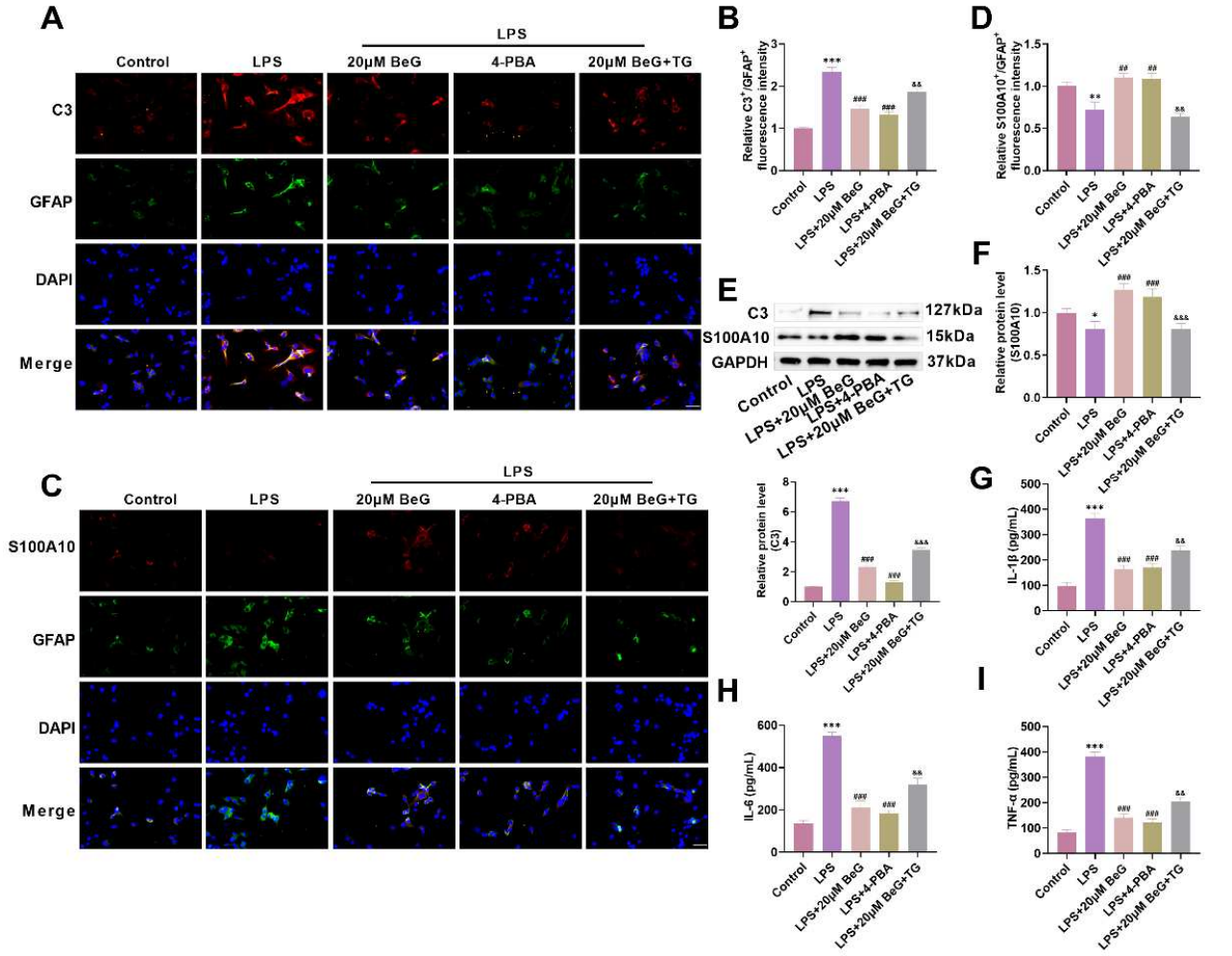

Fig. 4: BeG inhibits LPS-induced astrocyte A1 polarization by suppressing ERS.
(A-D) Five experimental groups (Control, LPS, LPS+20 μM BeG, LPS+4-PBA, LPS+20 μM BeG+TG) were established to evaluate ERS-mediated astrocyte polarization. Immunofluorescence quantified A1 ($GFAP^+/C3^+$) and A2 ($GFAP^+/S100A10^+$) subpopulations. Scale bar 50 μm. (E-F) Polarization markers (A1: C3; A2: S100A10) were quantified by immunoblotting. (G-I) Pro-inflammatory cytokines (IL-1β, IL-6, TNF-α) were measured via ELISA to assess neuroinflammatory modulation. n=3. ** P<0.01,*** P<0.001 vs Control; ## P<0.01, ### P<0.001 vs LPS; && P<0.01, &&& P<0.001 vs LPS+20 μM BeG.

Importantly, as key regulators of neuronal survival, growth and functional maintenance, the restoration of neurotrophic factor levels is crucial for neuroprotection (El Ouaamari *et al.*, 2023; Numakawa and Kajihara, 2025). This study demonstrated that BeG treatment could dose-dependently promote the restoration of the expression of important neurotrophic factors (BDNF, GDNF). The results propose that BeG could mediate neuroprotection through multiple pathways: inhibiting astrocyte activation induced by LPS, alleviating neuroinflammatory processes, shielding dopaminergic neurons from degeneration and enhancing neurotrophic factor recovery.

Research has demonstrated that reactive astrocytes exhibit functional heterogeneity and can be polarized into two distinct subtypes: neurotoxic A1 and neuroprotective A2 astrocytes (Sanchez *et al.*, 2021). A1 astrocytes are activated by microglia-derived pro-inflammatory factors, leading to increased expression of complement genes such as C3 and secretion of neurotoxic substances that contribute to neuronal damage. In contrast, A2 astrocytes are induced by ischemic conditions or growth factors and are characterized by elevated production of neurotrophic factors and antioxidant enzymes that promote neuronal survival and repair (Santiago-Balmaseda *et al.*, 2024). This polarization mechanism represents a promising therapeutic target for PD. In this study, LPS stimulation was found to promote A1 astrocyte polarization, as shown by increased C3 expression and decreased S100A10 levels. BeG treatment effectively counteracted this shift in a dose-dependent manner, suppressing C3 while enhancing S100A10 expression. Immunofluorescence analysis further verified that BeG reduced GFAP/C3 double-positive A1 astrocytes while increasing GFAP/S100A10 double-positive A2 cells.

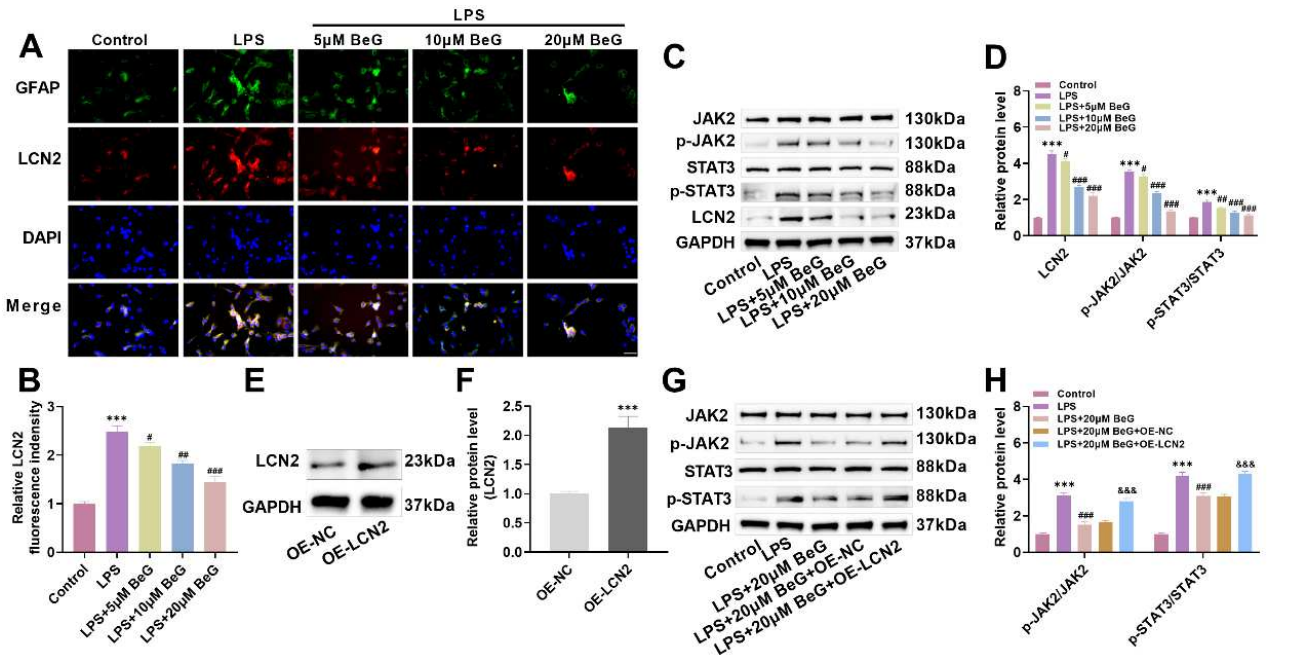

Fig. 5: BeG inhibits the LCN2/JAK2/STAT3 signaling pathway in LPS-induced astrocytes.
(A-B) Immunofluorescence colocalization of LCN2/GFAP evaluated BeG's modulation of the LCN2/JAK2/STAT3 axis in astrocytes. Scale bar 50 μm. (C-D) Immunoblotting quantified LCN2 and JAK2/STAT3 phosphorylation. (E-F) LCN2-overexpressing astrocytes were validated by immunoblot analysis. n=3. *** P<0.001 vs OE-NC. (G-H) Five groups (Control, LPS, LPS+20 μM BeG, LPS+BeG+OE-NC, LPS+BeG+OE-LCN2) were analyzed for JAK2/STAT3 pathway proteins to delineate BeG's mechanistic action. n=3. *** P<0.001 vs Control; # P<0.05, ## P<0.01, ### P<0.001 vs LPS; &&& P<0.001 vs LPS+20 μM BeG.

Importantly, these *in vitro* observations were consistently reproduced *in vivo*, strongly supporting the therapeutic potential of BeG. In summary, BeG not only effectively inhibits excessive activation of astrocytes, but also regulates their polarization state by suppressing A1-type polarization and promoting the conversion to the neuroprotective A2-type, thereby alleviating neurotoxicity, inhibiting neuroinflammation and ultimately exerting neuroprotective effects.

The ER maintains intracellular proteostasis through its pivotal roles in protein folding, modification and distribution. Accumulation of unfolded/misfolded proteins following ER dysfunction initiates ERS (Jiang *et al.*, 2021), prompting cells to activate the UPR mechanism as an adaptive response to reinstate ER homeostasis (Ong and Logue, 2023). In astrocytes, this conserved stress response mechanism manifests as follows: when the levels of unfolded proteins increase, the molecular chaperone GRP78/BiP dissociates from ER transmembrane receptors (PERK, ATF6 and IRE1α), thereby activating the UPR signaling pathway (Li *et al.*, 2022). Although the UPR protects cells by enhancing protein folding capacity and limiting new protein synthesis, persistent ERS and UPR activation in astrocytes may have opposite effects, failing to alleviate the stress and instead promoting pathological progression, thus accelerating the development of PD. More seriously, when ERS is excessive or prolonged, the UPR switches from an adaptive protective response to an apoptotic signaling pathway, ultimately leading to cell death (Wang *et al.*, 2023). This study confirmed that LPS stimulation significantly activates the ERS signaling pathway, specifically demonstrated by the upregulation of CHOP and GRP78 expression, as well as increased phosphorylation levels of IRE1α and PERK, indicating that neuroinflammation is accompanied by significant ERS. Moreover, LPS treatment also led to an increased apoptosis rate in astrocytes, as evidenced by an increased number of TUNEL-positive cells, upregulation of pro-apoptotic proteins and downregulation of the anti-apoptotic protein. Importantly, BeG treatment not only effectively reversed these pathological changes, thereby inhibiting LPS-induced astrocyte ERS and apoptosis. Furthermore, this study introduced ERS inhibitors (4-PBA) and agonists (TG) to further confirm that BeG specifically inhibits the ERS pathway to attenuate the polarization shift of astrocytes towards the A1 phenotype and reduce the secretion of inflammatory factors. LCN2 is significantly upregulated in various neurodegenerative diseases and is thought to participate in disease progression by amplifying neuroinflammatory responses (Qiu *et al.*, 2024). The JAK2/STAT3 pathway, when activated by LCN2, has been shown to drive inflammatory processes and cellular injury. In neuroinflammatory states, this signaling cascade becomes dysregulated, resulting in amplified cytokine release and glial hyperactivation - a cyclic mechanism that progressively aggravates neuronal pathology (Jain *et al.*, 2021; Sadri, 2025; Yongtai *et al.*, 2025).

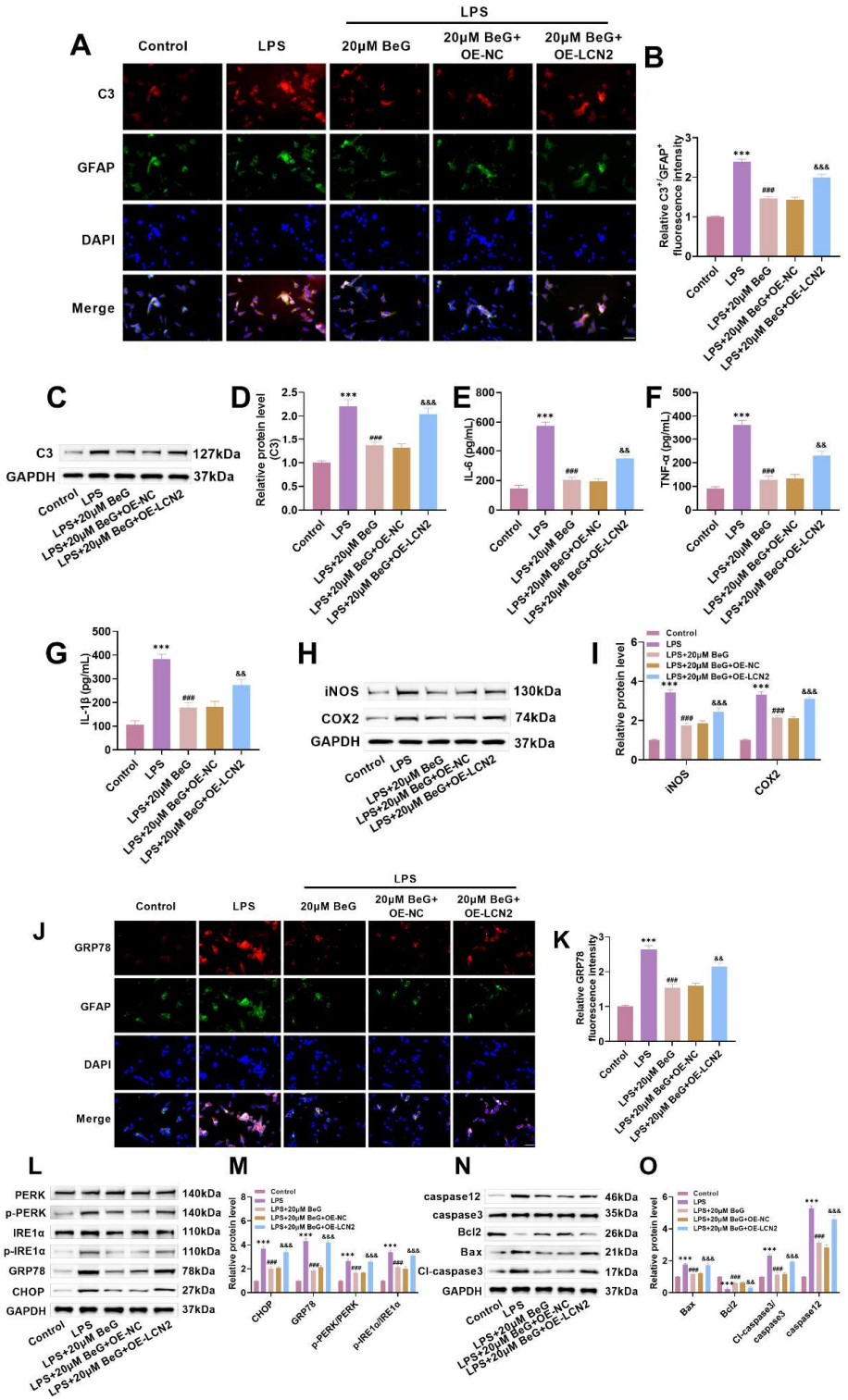

Fig. 6: BeG inhibits LPS-induced astrocyte activation, A1 polarization, and ERS by regulating the LCN2/JAK2/STAT3 pathway.

(A-B) GFAP and A1 marker C3 colocalization was assessed by immunofluorescence. Scale bar 50 μm. (C-D) C3 protein levels were quantified by immunoblotting. (E-G) Inflammatory cytokines (IL-1β, IL-6, TNF-α) were measured via ELISA. (H-I) Immunoblot analysis detected iNOS and COX2 expression. (J-K) GRP78/GFAP colocalization was visualized to evaluate ER stress. Scale bar 50 μm. (L-M) Key ER stress markers (CHOP, GRP78, IRE1α/p-IRE1α, PERK/p-PERK) were analyzed by immunoblotting. (N-O) Apoptotic regulators (Bax, Bcl-2, cleaved-caspase-3/caspase-3, caspase-12) were examined. n=3. *** P<0.001 vs Control; ### P<0.001 vs LPS; && P<0.01, &&& P<0.001 vs LPS+20 μM BeG.

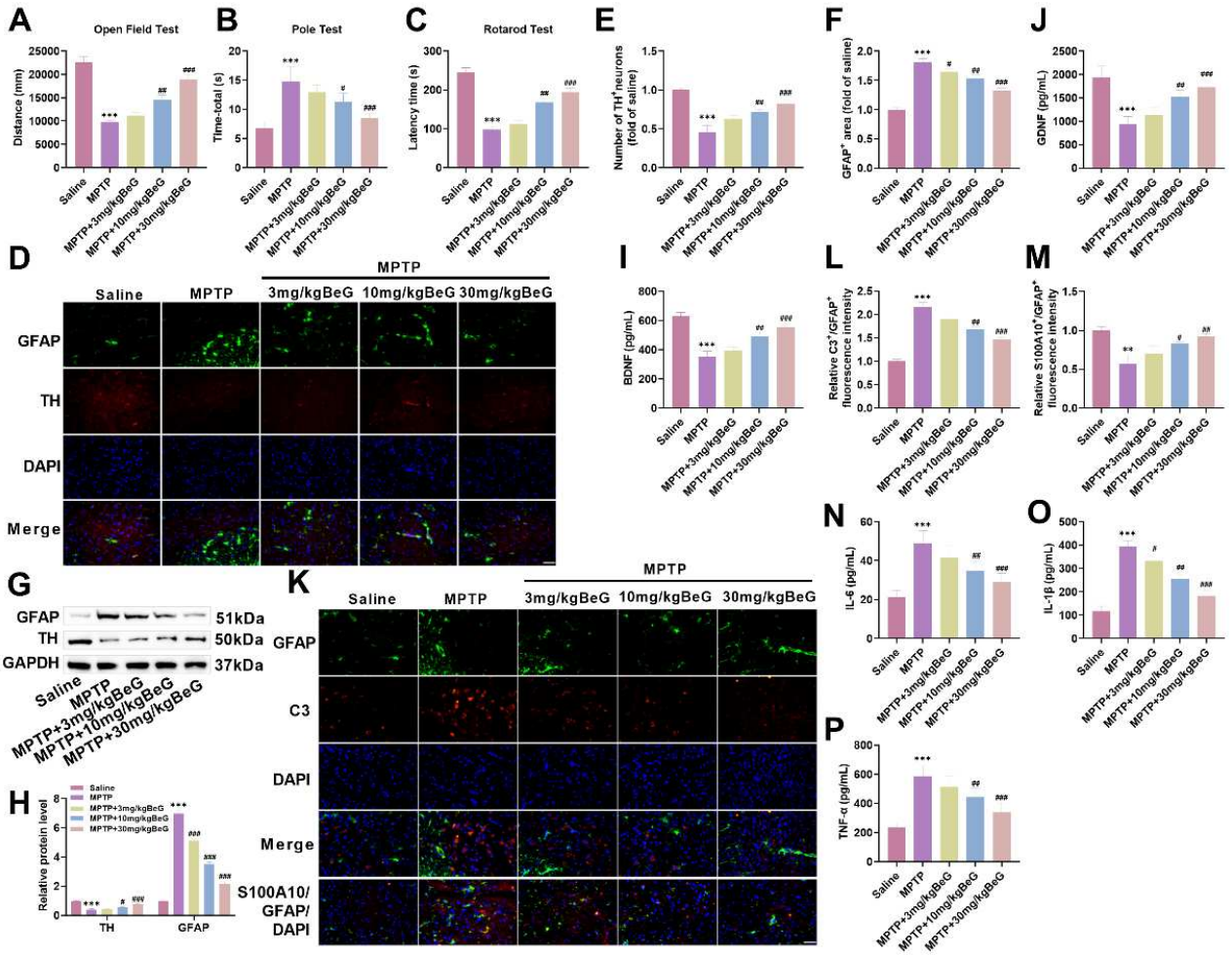

Fig. 7: BeG can inhibit astrocyte activation and A1 polarization in MPTP-induced PD mice.
(A-C) The neuroprotective efficacy of BeG was evaluated in an MPTP-induced PD mouse model with five treatment groups: Saline, MPTP and MPTP+BeG (3/10/30 mg/kg). Motor function was assessed using open field, pole, and rotarod tests. n=7. (D-F) GFAP/TH colocalization in substantia nigra was examined by immunofluorescence to evaluate neuron-glia interactions. Scale bar 50 μm. (G-H) GFAP and TH protein levels in brain tissue were quantified by immunoblotting. (I-J) Neurotrophic factors (BDNF, GDNF) were measured via ELISA. (K-M) Astrocyte polarization (C3/GFAP and S100A10/GFAP) was analyzed by immunofluorescence. Scale bar 50 μm. (N-P) Pro-inflammatory cytokines (IL-6, IL-1β, TNF-α) in brain tissue were quantified to assess neuroinflammation modulation. n=3. ** P<0.05, *** P<0.001 vs Control; # P<0.05, ## P<0.01, ### P<0.001 vs MPTP.

Emerging evidence highlights crosstalk between ERS and astrocytic inflammation, wherein PERK-dependent JAK1/STAT3 activation upregulates pro-inflammatory mediators (e.g., IL-6). The LCN2/JAK2/STAT3 pathway may thus contribute to PD progression by synchronizing ERS with neuroinflammatory responses (Wang *et al.*, 2021a). Our findings indicate that BeG inhibits LPS-triggered activation of the LCN2/JAK2/STAT3 axis. The critical involvement of LCN2 in BeG's mechanism was confirmed through gain-of-function experiments, where LCN2 overexpression partially restored JAK2/STAT3 activity and counteracted BeG's ability to modulate A1 astrocyte markers, cytokine production and inflammatory enzymes. More importantly, LCN2 overexpression also partially counteracted BeG's improvement of ERS markers (GRP78, CHOP expression and IRE1α/PERK phosphorylation) and apoptosis-related indicators. These results systematically reveal the key regulatory role of the LCN2/JAK2/STAT3 signaling axis in astrocyte-mediated neuroinflammation, ERS and cell apoptosis and clarify the molecular mechanism through which BeG exerts multiple neuroprotective effects by targeting this pathway. It provides important experimental evidence and theoretical support for the development of pathway-targeted therapeutic strategies for PD.

Although this study provides new experimental evidence and mechanistic insights into the application of BeG in the treatment of PD, there are still several limitations that warrant further investigation and refinement in future research. First, regarding the animal model, this study employed an MPTP-induced PD mouse model.

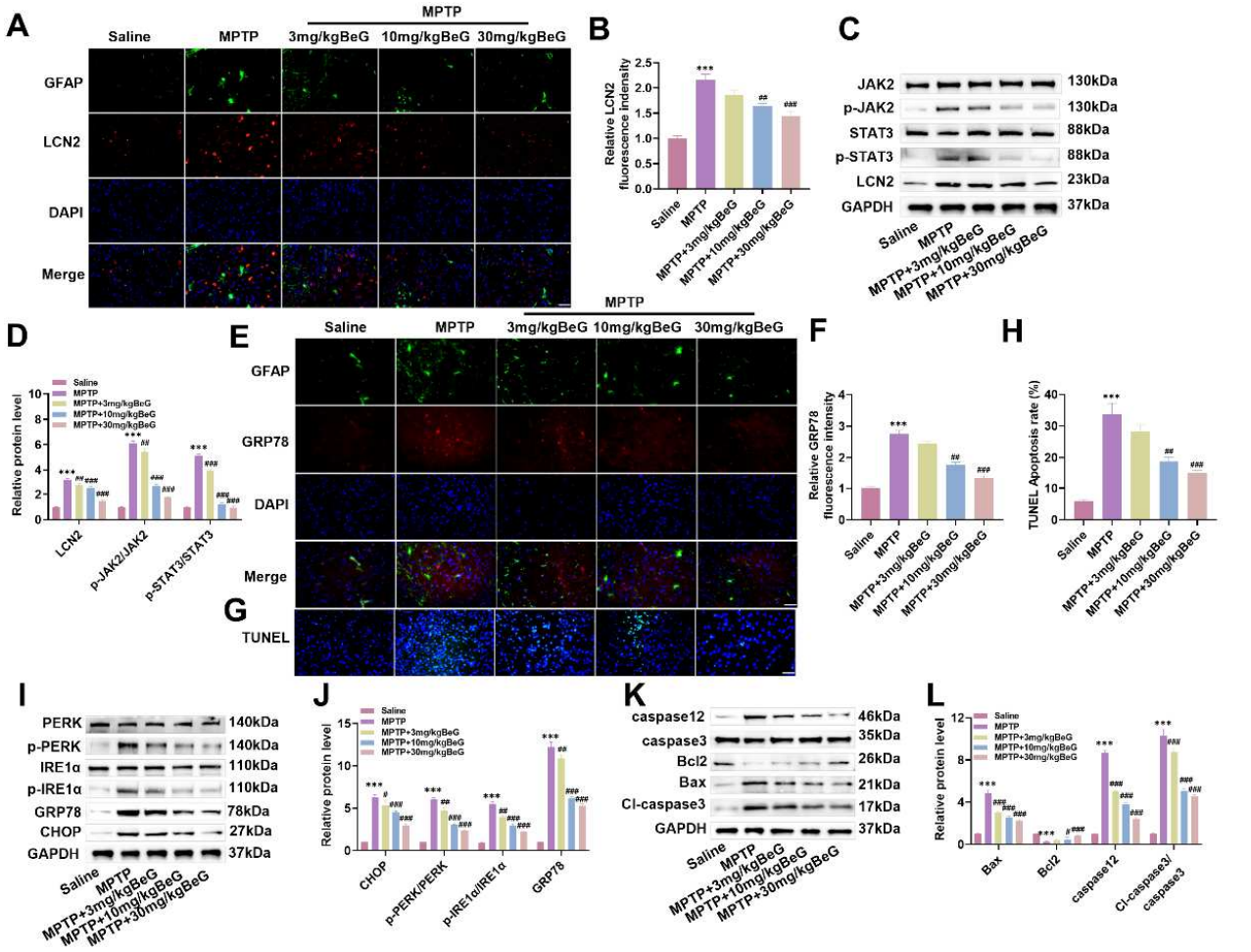

Fig. 8: BeG alleviates neuroinflammatory stress in MPTP-induced PD mice by inhibiting the LCN2/JAK2/STAT3 signaling pathway.

(A-B) LCN2/GFAP co-expression was analyzed by immunofluorescence. Scale bar 50 μm. (C-D) Immunoblotting quantified LCN2/JAK2/STAT3 pathway activation (LCN2, p-JAK2/JAK2, p-STAT3/STAT3). (E-F) GRP78/GFAP colocalization in brain tissue was assessed. Scale bar 50 μm. (G-H) Neuronal apoptosis was measured by TUNEL assay. Scale bar 50 μm. (I-J) ER stress markers (CHOP, GRP78, IRE1α/p-IRE1α, PERK/p-PERK) were examined. (K-L) Apoptotic regulators (Bax, Bcl-2, caspase-3/cleaved-caspase-3, caspase-12) were analyzed. n=3. *** P<0.001 vs Control; # P<0.05, ## P<0.01, ### P<0.001 vs MPTP.

Although this model is widely used in PD research (Mustapha and Taib, 2021), it is an acute model and may not fully recapitulate the complexity of the human PD disease course, which could affect the direct translatability of the findings to clinical practice. Second, in terms of the *in vitro* cell model, the study relied solely on an LPS-induced astrocyte activation model to simulate neuroinflammation. While this model effectively induces inflammatory responses, the pathological mechanisms of PD are highly complex and also involve factors such as abnormal aggregation of α-synuclein and mitochondrial dysfunction (Dong-Chen *et al.*, 2023). Future studies could incorporate more diverse pathological models, such as treating cells with α-synuclein aggregates, to more comprehensively mimic the actual pathological environment of PD and thereby enhance the translational relevance of the findings. Regarding the specificity of the mechanism of action, this study robustly demonstrated that BeG exerts neuroprotective effects via the LCN2/JAK2/STAT3 pathway. However, as a natural compound, BeG may have multi-target effects. The study did not fully exclude the possibility that other potential and parallel signaling pathways might also be involved in its neuroprotective process. Therefore, the conclusion that BeG acts primarily through this pathway requires further validation. Additionally, the relatively small sample size in this study may affect the statistical power and generalizability of the conclusions. Future research should consider using larger sample sizes to validate the current findings. Finally, this study lacks key data on the pharmacokinetics of BeG (such as absorption, distribution, metabolism and excretion), long-term safety and its blood-brain barrier permeability within the brain. These pieces of information are critical for evaluating its clinical feasibility as a potential therapeutic agent.

CONCLUSION

This study demonstrates that BeG inhibits the LCN2/JAK2/STAT3 pathway, suppressing A1-type astrocyte activation while reducing ER stress and apoptosis. These neuroprotective effects improve PD-like behavioral deficits, supporting BeG's therapeutic potential and highlighting LCN2/JAK2/STAT3 as a promising PD treatment target. Although our research focuses on astrocytic regulation by BeG, the complex nature of PD involves diverse cellular components. Additional investigations are needed to evaluate BeG's direct impact on other neural cells, particularly microglia and neurons.

Acknowledgment
None

Author's contribution
Jiaxin Li: Conceived and designed the research, conducted experiments and analyzed data. Drafted and revised the manuscript critically for important intellectual content.
Rui Tang: Contributed to the acquisition, analysis and interpretation of data. Provided substantial intellectual input during the drafting and revision of the manuscript.
Jiahui Liu: Participated in the conception and design of the study. Played a key role in data interpretation and manuscript preparation.
All authors have read and approved the final version of the manuscript.

Funding
Mechanistic study on the improvement of Parkinson's disease by TRPV1 through AMPK activation via CaMKII. (No. 2025MS08114)

Data availability statement
The datasets generated and analysed during the current study are available from the corresponding author on reasonable request.

Ethical approval
All procedures were performed in compliance with institutional animal care standards and were approved by the Ethics Committee (No. SY20241107, dated: 2024.11.20).

Conflict of interest
The authors declare that they have no conflicts of interest.

REFERENCES

Bloem BR, Okun MS and Klein C (2021). Parkinson's disease. *Lancet*, **397**(10291): 2284-2303.

Boulton M and Al-Rubaie A (2025). Neuroinflammation and neurodegeneration following traumatic brain injuries. *Anat. Sci. Int*., **100**(1): 3-14.

Brash-Arias D, Garcia LI, Perez-Estudillo CA, Rojas-Duran F, Aranda-Abreu GE, Herrera-Covarrubias D and Chi-Castaneda D (2024). The role of astrocytes and alpha-synuclein in parkinson's disease: A review. *NeuroSci*., **5**(1): 71-86.

Chen YJ, Xie MR, Zhou SQ and Liu F (2025). Astrocytes-associated research in Parkinson's disease: An explored trends analysis. *Front. Aging Neurosci.*, **17**: 1563142.

Ding ZB, Song LJ, Wang Q, Kumar G, Yan YQ and Ma CG (2021). Astrocytes: A double-edged sword in neurodegenerative diseases. *Neural Regener. Res.*, **16**(9): 1702-1710.

Dong-Chen X, Yong C, Yang X, Chen-Yu S and Li-Hua P (2023). Signaling pathways in Parkinson's disease: Molecular mechanisms and therapeutic interventions. *Signal Transduction Targeted Ther*., **8**(1): 73.

Dong AQ, Yang YP, Jiang Sm, Yao XY, Qi D, Mao Cj, Cheng XY, Wang F, Hu LF and Liu CF (2023). Pramipexole inhibits astrocytic NLRP3 inflammasome activation via Drd3-dependent autophagy in a mouse model of Parkinson's disease. *Acta Pharmacol. Sin.*, **44**(1): 32-43.

Dorsey ER and Bloem BR (2024). Parkinson's disease is predominantly an environmental disease. *J Parkinsons Dis*., **14**(3): 451-465.

El Ouaamari Y, Van den Bos J, Willekens B, Cools N and Wens I (2023). Neurotrophic factors as regenerative therapy for neurodegenerative diseases: Current status, challenges and future perspectives. *Int. J. Mol. Sci.*, **24**(4): 3866.

Fan Y, Maghimaa M, Chinnathambi A, Alharbi S A, Veeraraghavan VP, Mohan SK, Hussain S and Rengarajan T (2021). Tomentosin reduces behavior deficits and neuroinflammatory response in MPTP-induced Parkinson's disease in mice. *J. Environ. Pathol., Toxicol. Oncol.*, **40**(1): 75-84.

Gao A, McCoy HM, Zaman V, Shields DC, Banik NL and Haque A (2022). Calpain activation and progression of inflammatory cycles in Parkinson's disease. *Front. Biosci.-Landmark*., **27**(1): 20.

Gonzalez-Latapi P, Bayram E, Litvan I and Marras C (2021). Cognitive impairment in Parkinson's disease: Epidemiology, clinical profile, protective and risk factors. *Behav. Sci*., **11**(5): 74.

Han B, An Z, Gong T, Pu Y and Liu K (2024). LCN2 promotes proliferation and glycolysis by activating the JAK2/STAT3 signaling pathway in hepatocellular carcinoma. *Appl. Biochem. Biotechnol*., **196**(2): 717-728.

Haque ME, Azam S, Akther M, Cho DY, Kim IS and Choi DK (2021). The neuroprotective effects of GPR4 inhibition through the attenuation of caspase mediated apoptotic cell death in an MPTP induced mouse model of Parkinson's disease. *Int. J. Mol. Sci.*, **22**(9): 4674.

Hart C G, Karimi-Abdolrezaee S (2021). Recent insights on astrocyte mechanisms in CNS homeostasis, pathology and repair. *J. Neurosci. Res*., **99**(10): 2427-2462.

Jain M, Singh M K, Shyam H, Mishra A, Kumar S, Kumar A and Kushwaha J (2021). Role of JAK/STAT in the neuroinflammation and its association with neurological disorders. *Ann. Neurosci*., **28**(3-4): 191-200.

Jiang Y, Tao Z, Chen H and Xia S (2021). Endoplasmic reticulum quality control in immune cells. *Front. Cell Dev. Biol*., **9**: 740653.

Jung BK, Park Y, Yoon B, Bae JS, Han SW, Heo JE, Kim DE and Ryu KY (2023). Reduced secretion of LCN2 (lipocalin 2) from reactive astrocytes through autophagic and proteasomal regulation alleviates inflammatory stress and neuronal damage. *Autophagy*., **19**(8): 2296-2317.

Jung BK and Ryu KY (2023). Lipocalin-2: A therapeutic target to overcome neurodegenerative diseases by regulating reactive astrogliosis. *Exp. Mol. Med*., **55**(10): 2138-2146.

Jurcau A, andronie-Cioara FL, Nistor-Cseppento DC, Pascalau N, Rus M, Vasca E and Jurcau MC (2023). The involvement of neuroinflammation in the onset and progression of Parkinson's disease. *Int. J. Mol. Sci.*, **24**(19): 14582.

Jurga AM, Paleczna M, Kadluczka J, Kuter KZ (2021). Beyond the GFAP-astrocyte protein markers in the brain. *Biomolecules*., **11**(9): 1361.

Kim S, Pajarillo E, Nyarko-Danquah I, Aschner M, Lee E (2023). Role of astrocytes in Parkinson's disease associated with genetic mutations and neurotoxicants. *Cells*., **12**(4): 622.

Kwon DK, Kwatra M, Wang J and Ko HS (2022). Levodopa-induced dyskinesia in Parkinson's disease: Pathogenesis and emerging treatment strategies. *Cells*., **11** (23), 3736.

Lee H-G, Wheeler M A and Quintana F J (2022). Function and therapeutic value of astrocytes in neurological diseases. *Nat. Rev. Drug Discovery*., **21**(5): 339-358.

Li J, Hussain S A, Daddam J R and Sun M (2025a). Bergapten attenuates human papillary thyroid cancer cell proliferation by triggering apoptosis and the GSK-3β, P13K and AKT pathways. *Adv. Clin. Exp. Med*., **34**(1): 113-122.

Li X, Hu F, Lu T, Wu S, Ma G, Lin Y and Zhang H (2025b). Endoplasmic reticulum stress in non-small cell lung cancer. *Am. J. Cancer Res.*, **15**(4): 1829.

Li Y, Lu L, Zhang G, Ji G and Xu H (2022). The role and therapeutic implication of endoplasmic reticulum stress in inflammatory cancer transformation. *Am. J. Cancer Res*., **12**(5): 2277.

Liang Y, Xie L, Liu K, Cao Y, Dai X, Wang X, Lu J, Zhang X and Li X (2021). Bergapten: A review of its pharmacology, pharmacokinetics and toxicity. *Phytother. Res.*, **35**(11): 6131-6147.

Liu X, Hussain R, Mehmood K, Tang Z, Zhang H and Li Y (2022). Mitochondrial-endoplasmic reticulum communication-mediated oxidative stress and autophagy. *BioMed Res. Int.*, **2022**(1): 6459585.

Mulroy E, Erro R, Bhatia KP and Hallett M (2024). Refining the clinical diagnosis of Parkinson's disease. *Parkinsonism Relat. Disord*., **122**, 106041.

Mustapha M, Taib CNM (2021). MPTP-induced mouse model of Parkinson's disease: A promising direction for therapeutic strategies. *Bosnian J. Basic Med. Sci*., **21**(4): 422.

Nourbakhsh M, Sharifi R, Heydari N, Nourbakhsh M, Ezzati-Mobasser S and Zarrinnahad H (2022). Circulating TRB3 and GRP78 levels in type 2 diabetes patients: crosstalk between glucose homeostasis and endoplasmic reticulum stress. *J. Endocrinol. Invest*., pp.1-7.

Numakawa T and Kajihara R (2025). The role of brain-derived neurotrophic factor as an essential mediator in neuronal functions and the therapeutic potential of its mimetics for neuroprotection in neurologic and psychiatric disorders. *Molecules*., **30**(4): 848.

Ong G and Logue SE (2023). Unfolding the interactions between endoplasmic reticulum stress and oxidative stress. *Antioxidants*., **12**(5): 981.

Ou Z, Pan J, Tang S, Duan D, Yu D, Nong H and Wang Z (2021). Global trends in the incidence, prevalence and years lived with disability of Parkinson's disease in 204 countries/territories from 1990 to 2019. *Front. Public Health*., **9**: 776847.

Pang QM, Chen SY, Xu QJ, Fu SP, Yang YC, Zou WH, Zhang M, Liu J, Wan WH and Peng JC (2021). Neuroinflammation and scarring after spinal cord injury: Therapeutic roles of MSCs on inflammation and glial scar. *Front. Immunol*., **12**: 751021.

Parkkinen I, Their A, Asghar M Y, Sree S, Jokitalo E and Airavaara M (2023). Pharmacological regulation of endoplasmic reticulum structure and calcium dynamics: Importance for neurodegenerative diseases. *Pharmacol. Rev*., **75**(5): 959-978.

Perri M R, Pellegrino M, Aquaro S, Cavaliere F, Lupia C, Uzunov D, Marrelli M, Conforti F and Statti G (2022). Cachrys spp. from Southern Italy: Phytochemical characterization and JAK/STAT signaling pathway inhibition. *Plants*., **11**(21): 2913.

Pierre WC, Londono I, Quiniou C, Chemtob S and Lodygensky GA (2022). Modulatory effect of IL-1 inhibition following lipopolysaccharide-induced neuroinflammation in neonatal microglia and astrocytes. *Int. J. Dev. Neurosci*., **82**(3): 243-260.

Qiao CM, Tan LL, Ma XY, Xia YM, Li T, Li MA, Wu J, Nie X, Cui C and Zhao WJ (2025). Mechanism of S100A9-mediated astrocyte activation via TLR4/NF-κB in Parkinson's disease. *Int. Immunopharmacol*., **146**: 113938.

Qiu R, Cai Y, Su Y, Fan K, Sun Z and Zhang Y (2024). Emerging insights into Lipocalin-2: Unraveling its role in Parkinson's Disease. *Biomed. Pharmacother.*, **177**: 116947.

Qu Y, Li J, Qin Q, Wang D, Zhao J, An K, Mao Z, Min Z, Xiong Y and Li J (2023). A systematic review and meta-analysis of inflammatory biomarkers in Parkinson's

disease. *NPJ Parkinson's Dis.*, **9**(1): 18.

Rauf A, Badoni H, Abu-Izneid T, Olatunde A, Rahman M M, Painuli S, Semwal P, Wilairatana P and Mubarak MS (2022). Neuroinflammatory markers: Key indicators in the pathology of neurodegenerative diseases. *Molecules*., **27**(10): 3194.

Ren H, Zhai W, Lu X and Wang G (2021). The cross-links of endoplasmic reticulum stress, autophagy and neurodegeneration in Parkinson's disease. *Front. Aging Neurosci*. **13**: 691881.

Sadri F (2025). PROTACs in Colorectal Cancer: A new era in targeted protein degradation therapy. *Adv. Clin. Pharmacol. Ther.*, **2**(1): 1-16.

Sanchez A, Morales I, Rodriguez-Sabate C, Sole-Sabater M and Rodriguez M (2021). Astrocytes, a promising opportunity to control the progress of Parkinson's disease. *Biomedicines*., **9**(10): 1341.

Santiago-Balmaseda A, Aguirre-Orozco A, Valenzuela-Arzeta IE, Villegas-Rojas MM, Pérez-Segura I, Jiménez-Barrios N, Hurtado-Robles E, Rodríguez-Hernández LD, Rivera-German ER and Guerra-Crespo M (2024). Neurodegenerative Diseases: Unraveling the heterogeneity of astrocytes. *Cells*, **13**(11): 921.

Silva ABRL, De Oliveira RWG, Diógenes GP, De Castro Aguiar MF, Sallem CC, Lima MPP, De Albuquerque Filho LB, De Medeiros SDP, De Mendonça LLP De Santiago Filho PC (2023). Premotor, nonmotor and motor symptoms of Parkinson's disease: A new clinical state of the art. *Ageing Res. Rev.*, **84**: 101834.

Sims SG, Cisney RN, Lipscomb MM and Meares GP (2022). The role of endoplasmic reticulum stress in astrocytes. *Glia*., **70**(1): 5-19.

Song L, Wu Y, Yin L, Duan Y, Hua J, Rong M, Liu K, Yin J, Ma D and Zhang C (2025). Hydroxysafflower yellow A alleviates the inflammatory response in astrocytes following cerebral ischemia by inhibiting the LCN2/STAT3 feedback loop. *Metab. Brain Dis.*, **40**(4): 161.

Song Q, Peng S and Zhu X (2021). Baicalein protects against MPP+/MPTP-induced neurotoxicity by ameliorating oxidative stress in SH-SY5Y cells and mouse model of Parkinson's disease. *Neurotoxicology*., **87**: 188-194.

Su W, Liu H, Jiang Y, Li S, Jin Y, Yan C and Chen H (2021). Correlation between depression and quality of life in patients with Parkinson's disease. *Clin. Neurol. Neurosurg.*, **202**: 106523.

Subedi L, Gaire B P, Kim SY and Parveen A (2021). Nitric oxide as a target for phytochemicals in anti-neuroinflammatory prevention therapy. *Int. J. Mol. Sci*., **22**(9): 4771.

Tan Q, Zhang C, Rao X, Wan W, Lin W, Huang S, Ying J, Lin Y and Hua F (2024). The interaction of lipocalin-2 and astrocytes in neuroinflammation: Mechanisms and therapeutic application. *Front. Immunol*., **15**: 1358719.

Tripodi G, Lombardo M, Kerav S, Aiello G, Baldelli S (2025). Nitric oxide in parkinson's disease: The potential role of dietary nitrate in enhancing cognitive and motor health via the nitrate–nitrite–nitric oxide pathway. *Nutrients*., **17**(3): 393.

Vijiaratnam N, Simuni T, Bandmann O, Morris HR and Foltynie T (2021). Progress towards therapies for disease modification in Parkinson's disease. *Lancet Neurol*., **20**(7): 559-572.

Wang C, Yang T, Liang M, Xie J and Song N (2021a). Astrocyte dysfunction in Parkinson's disease: From the perspectives of transmitted α-synuclein and genetic modulation. *Transl. Neurodegener.*, **10**: 1-17.

Wang D, Qu S, Zhang Z, Tan L, Chen X, Zhong HJ and Chong CM (2023). Strategies targeting endoplasmic reticulum stress to improve Parkinson's disease. *Front. Pharmacol.*, **14**: 1288894.

Wang X, Li X, Zuo X, Liang Z, Ding T, Li K, Ma Y, Li P, Zhu Z and Ju C (2021b). Photobiomodulation inhibits the activation of neurotoxic microglia and astrocytes by inhibiting Lcn2/JAK2-STAT3 crosstalk after spinal cord injury in male rats. *J. Neuroinflammation.*, **18**(1): 256.

Wei Y, Chen T, Bosco D B, Xie M, Zheng J, Dheer A, Ying Y, Wu Q, Lennon VA and Wu LJ (2021). The complement C3-C3aR pathway mediates microglia–astrocyte interaction following status epilepticus. *Glia*., **69**(5): 1155-1169.

Wei ZYD and Shetty AK (2021). Treating Parkinson's disease by astrocyte reprogramming: Progress and challenges. *Sci. Adv.*, **7**(26): eabg3198.

Yan M, Bo X, Zhang J, Liu S, Li X, Liao Y, Liu Q, Cheng Y and Cheng J (2023). Bergapten alleviates depression-like behavior by inhibiting cyclooxygenase 2 activity and NF-κB/MAPK signaling pathway in microglia. *Exp. Neurol*., **365**: 114426.

Yang J, Dong J, Li H, Gong Z, Wang B, Du K, Zhang C, Bi H, Wang J, Tian X and Chen L (2024). Circular RNA HIPK2 promotes A1 astrocyte activation after spinal cord injury through autophagy and endoplasmic reticulum stress by modulating miR-124-3p-mediated Smad2 repression. *ACS Omega.*, **9**: 781-797.

Yang Q, Zhuang C (2025). Research progress on the role of exercise-regulated reactive astrocytes in the prevention and treatment of Parkinson's disease. *Front. Aging Neurosci*., **17**: 1561006.

Yongtai Z, Zhenyu Y, Yan L, Jiajing W and Bo Z (2025). Research progress on the mechanism of lipocalin-2 in neurological diseases. *Med. J. Peking Union Med. Coll. Hosp*., **16**(2): 330-337.

Zhong QQ and Zhu F (2022). Trends in prevalence cases and disability-adjusted life-years of Parkinson's disease: Findings from the global burden of disease study 2019. *Neuroepidemiology*., **56**(4): 261-270.